5th ECPMG Delft · 2024

Proceedings of the 5th ECPMG 2024
5th European Conference on Physical Modelling in Geotechnics
2-4 October 2024, Delft, the Netherlands

Examining levee integrity: centrifuge modelling of internal erosion arising from structural culvert defects

J. Westcott
Engineering Research and Development Center (ERDC), Vicksburg, MS, U.S., joelle.a.westcott@erdc.dren.mil

A.J. Bowman, A.C. Trautz, J.W. Murphy
Engineering Research and Development Center (ERDC), Vicksburg, MS, U.S., april.j.bowman@erdc.dren.mil, andrew.c.trautz@erdc.dren.mil, john.w.murphy@erdc.dren.mil

C. Karam
Virginia Tech, Blacksburg, VA, U.S., mkcarole@vt.edu

ABSTRACT: This paper presents pore pressure results following the hydro-mechanical response of levee systems, with a specific focus on internal erosion, a critical concern identified by the U.S. Army Corps of Engineers. Leveraging the Engineer Research and Development Centre's Centrifuge Research Complex, four 20G centrifuge tests were conducted, simulating different culvert defect scenarios. The experiments quantified the initiation, progression, and surface expression of internal erosion caused by these defects. The experimental design included the construction of a levee cross section with a 50.8mm diameter aluminium culvert, and the novel addition of thermal infrared sensing for detecting seepage and erosion channels. The integration of numerical modelling using SEEP/W successfully approximated steady-state conditions before the defect was opened. The experiments underscore the importance of addressing potential levee vulnerabilities given variations in measured pressure during the internal erosion process. The results also highlight the promising role of thermal infrared sensing in detecting seepage, suggesting its potential for future modelling applications. Further investigations involving systematic variation of boundary conditions and careful consideration of instrument proximity are recommended to enhance the understanding of the presented work.

1 INTRODUCTION

According to the U.S. National Levee Database, there are approximately 22,530km (14,000mi) of levees nationwide with 17,000 pipes, culverts, and conduits running through them (USACE, 2018). A culvert is a large circular or box-like covered hydraulic structure which conveys fluid, promotes drainage, and prevents ponding beneath a levee. These structures contribute to seepage issues and risk in approximately 40% of levee systems (USACE, 2018). There is a desire within the United States Army Corps of Engineers (USACE) to quantify the consequences of internal erosion caused by culvert defects in such systems.

Several studies have used centrifuge modeling to investigate hydraulic structures (e.g., Nakashima et al., 2020, Hudacsek 2009), which have provided valuable insight on pore pressure generation and displacement of the system under an increased acceleration field. In this paper, centrifuge modelling was used to assess the hydro-mechanical response of a levee system, focusing on pore pressure generation, soil cavity formation, and observable surficial deformation. This work soley focused on internal erosion into a pipe (PFM-3), one of seven common culvert failure modes (USACE, 2020).

2 EXPERIMENT DESIGN

A series of three 20G centrifuge tests were conducted at the recently rennovated Engineer Research and Development Center's (ERDC) Centrifuge Research Complex (CRC). The ERDC CRC centrifuge has a 1,200 g-ton capacity and a 6.5m radius (Bowman et al., 2022).

The experiment modelled internal erosion into a culvert where surrounding soil erodes into structural defects. Culvert defects can be caused by improperly installed connections, crushed culvert sections, or by corrosion causing a hole to form. The movement of embankment material into the defect can be driven by normal precipitation, infilitration, or hydraulic loading events such as floods (Figure 1).

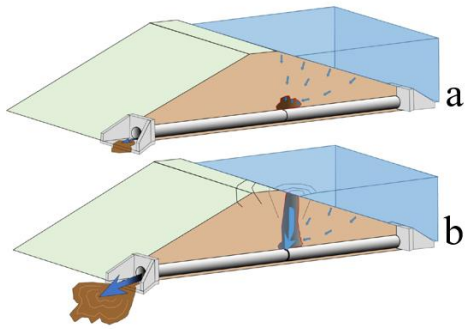

Figure 1. Internal erosion mechanism into a culvert structure (USACE, 2020). a) An erosion channel forms within the embankment as soil flows into the culvert defect. b) The erosion channel reaches the water source and initiates uncontrolled flow.

Taking advantage of the symmetry of the problem, a two dimensional cross section of the levee and culvert was created and placed against an acrylic window as shown in Figure 2. This allowed visual analysis methods to be used. Table 1 outlines the four centrifuge tests, distinguishing the culvert defect location and size in model scale. The culvert defect location was measured from the upstream toe of the levee to the center of the defect. The defect size for Test 1 represents a smaller defect or misalignment at a culvert joint while the defect size for Tests 2-4 represent a collapse of a culvert section.

Table 1. Centrifuge test number with corresponding culvert defect location and size in model scale.

Test Number	Defect Location (mm)	Defect Size l x w (mm)	Drainage Through Culvert?
1	390	10 x 10	Y
2	390	40 x 15	Y
3	195	40 x 15	Y
4	390	40 x 15	N

2.1 Container Design

A window box with a length, height, and width of 1270mm x 482mm x 335mm was used for these experiments (Figure 2). The tank contained a false bottom below the model to store and supply the water necessary for conducting the experiment. Opposite the window, a Teknic motor drove a pump which circulated the water during the test. A manifold was used to diffuse the water, eliminating surface erosion at the upstream toe. Sediment traps were placed at the bottom of the container to limit potential blockage at the pump intake. The downstream end of the levee was supported by a vertical perforated plate which allowed for drainage without loss of soil material.

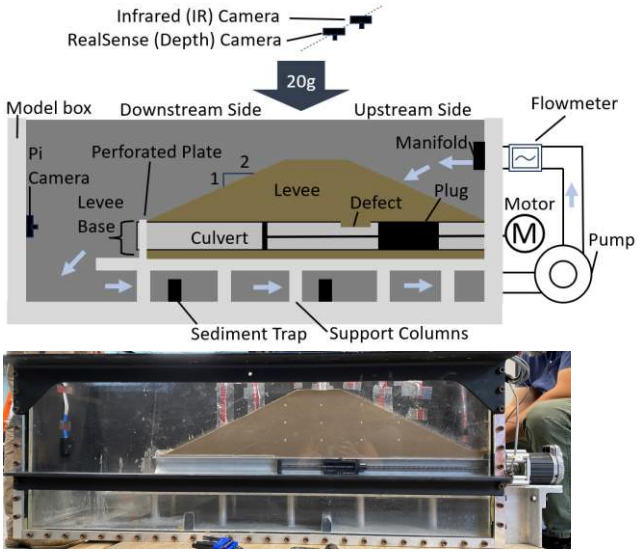

Figure 2. Diagram and image of the container, built levee, culvert, 3D printed plug, ball screw, and motor.

2.2 Culvert Design

A 50.8mm diameter aluminum culvert was used for the centrifuge model, scaling to a 1.02m (40in) prototype. The culvert size was chosen to meet the USACE recommended minimum culvert diameters of 91.4 - 121.9cm (36 - 48in) at prototype scale (USACE, 2020) and to allow for the insertion of a 3D-printed plug connected to a ball screw and second motor. The plug was printed with Phrozen`s Aqua Gray-8K Resin. The culvert was installed and sealed against the glass with marine grade silicone.

The plug was used to block the culvert defect, limiting flow into the culvert until target centrifugal acceleration and levee saturation were reached. The sides of the plug, abutting the window and against the inside of the culvert, contained four parallel tracks of 3.175mm (0.125in) ball bearings. These were used to reduce the friction of the plug against the window and pipe during retraction. Vacuum grease was applied to the culvert to lubricate the plug, improving its movement, and eliminating seepage into the defect prematurely.

2.3 Levee Construction

A manufactured silty sand (SM) with 70% 40/70 sand, 25% silt, and 5% clay was created for these tests. This material was chosen due to its similarity to field levees in terms of soil type and hydraulic conductivity (USACE, 2018). An average hydraulic conductivity of 6.33×10^{-5}m/s was determined from a series of falling head tests on compacted soil samples.

Following similar procedures to levee field construction, the soil was compacted at its optimum water content of 7.5% to a relative density of 95%

based on modified proctor tests. An 84mm thick layer of soil was placed around the culvert and served as a base for the levee. Soil was added to this base layer in 25mm lifts, creating a 200mm tall levee with a 2:1 slope. This replicates a 4m (13.1ft) tall levee at the prototype scale (Figure 3).

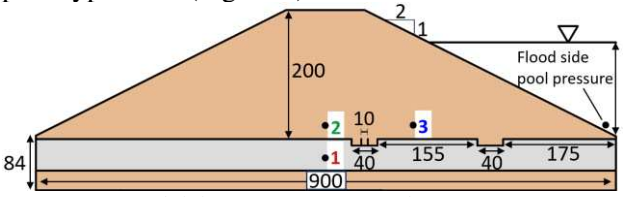

Figure 3. Model levee geometry, culvert cross sections, and PPT locations. All dimensions, indicated by arrows, are in mm.

2.4 Instrumentation

Pore pressure transducers (PPTs) were used to assess the saturation of the levee (Figure 3). The pore pressure sensors were placed in the centre of the levee section, 160mm from glass for tests 1-3, and placed 50mm from the glass in test 4. A Version 2 Raspberry Pi camera was used to visually monitor the cross section of the levee through the window (not drawn in diagrams) meanwhile, a second pi camera focused on the downstream levee face and culvert outflow. A RealSense D455 Depth Camera was mounted above the model to measure surficial deformation of the levee (Figure 2). This stereo camera was only used in Tests 1, 2 and 4 when the anticipated surface deformation was not located beneath the water.

A thermal infrared (IR) camera was also incorporated into the experimental design, a novel instrument for the centrifuge model. IR cameras are used in a range of industries and often identify anomalies based on radiation/temperature contrasts (Vollmer & Möllmann, 2018). Thermal infrared was introduced to remotely track seepage and possibly identify the locations of active erosion therefore exact temperature values were not the focus of the IR cameras. Two different models were tested, a FLIR Boson ADK camera (used for Test 1 and 2) and an ICI Helios 640 (used for Test 4). Both cameras detect longwave infrared (LWIR) radiation between 8-14µm. Requisite thermal contrast was created by cooling the water with ice to 10.6^{0}C (51^{0}F) prior to the start of the experiment. Although hydraulic processes can be influenced by temperature, the effect of the cooled water on the internal erosion process was assumed to be insignificant. Figure 4 provides plan views of the centrifuge levee experiment in RGB from the RealSense (top) and thermal IR from the Helios 640 (bottom). In the LWIR image, the light blue corresponds to the cool water introduced to the model mid-flight during the experiment and dark blue, the chilled soil with the waterline dividing the two regions.

Analysis of the IR imagery in all tests show that seepage could be detected along the model perimeter where flow preferentially occurred. Close analysis of the thermal images, of both the Boson ADK and the Helios 640 used in Tests 2 and 4 respectively, shows that the thermal signature of the erosion channel could be detected just prior to it becoming visible at the soil surface. Such observations could not be observed in the RGB imagery. Both infrared cameras performed adequately, identifying the temperature anomalies in the seepage path; however, for brevity, only the IR camera imagery from the Helios 640 is presented because it produced a higher resolution image (Figure 4). These results demonstrate that thermal infrared sensing could be a useful tool in centrifuge modelling, warranting further testing and exploration of its potential uses. Outside of the centrifuge, LWIR camera technology may be a promising inspection tool in the field. However, more testing under real world atmospheric conditions would be required.

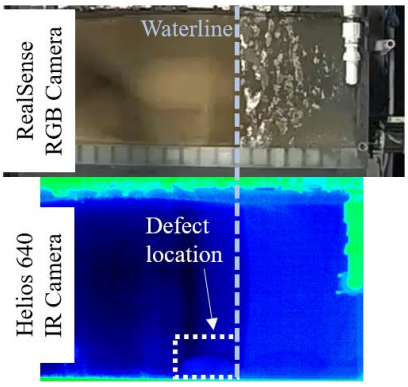

Figure 4. (Top) RGB image of levee experiment, plan view (Bottom) IR image from Helios 640, Test 4 at about 95% the time until surface manifestation. The ROI defined by the white box depicts the erosion channel prior to surface visibility.

3 TEST PROCEDURE

Once the target acceleration of 20g was reached, water was pumped into the centrifuge model to a height of 145mm. The pump rate was adjusted to account for infiltration into the soil to maintain this height throughout the experiment.

Once the levee was saturated, as determined from the PPT readings and Rasberry Pi camera, the defect in the culvert was exposed by retracting the plug. This caused the flow to be directed preferentially into the culvert and initialize erosion. The water level was maintained on the upstream side of the levee for 60 minutes or until the erosion channel propagated to the surface.

4 NUMERICAL MODELING

As part of the preliminary test design, and as a general comparison tool, the results from a finite element SEEP/W model were used to compare against experimental data.

4.1 Numerical Model Design and Set-Up

A two-dimensional numerical model, replicating a levee at prototype scale, was created for the computational component of this study. A global mesh size of 0.2m was used to ensure each 4-point quadrilateral element was no larger than the smallest culvert defect size (0.2m at prototype scale). This resulted in a total of 3916 elements and 4050 nodes.

The levee system, before the defect exposure, was modelled. The numerical model was used to identify the phreatic surface and pore pressures at system equilibrium (i.e. steady state). The top of the culvert was used as the bottom boundary of the model. An impermeable Neumann-type boundary condition was applied to the base, crest, and upper region of the upstream face. The downstream face of the levee was assigned a free surface (zero pressure) Dirichlet boundary condition. A constant head Dirichlet boundary condition of 2.9m was assigned to the upstream face of the levee in contact with the free water. Geometry, mesh, and the applied boundary conditions are presented in Figure 5.

A saturated-only material model (GeoStudio, 2022) was used for the SM soil, which links volumetric straining of the soil structure to pore-water pressure variation during transient analysis. However, in this case for steady state analysis, the storage parameters reduce to zero. Table 2 outlines the soil parameters and their corresponding values. SEEP/W, assuming saturated conditions, was used to simulate steady-state seepage (i.e., until the system has reached equilibrium) within the levee. The reader is referred to Table 2 for the values of key parameters assigned to the model.

Table 2. Soil parameters for saturated only material model

Parameter	Symbol	Value	Unit
Hydraulic Conductivity	K_{sat}	6.3x10^{-5}	m/s
Soil structure compressibility	β	1x10^{-5}	m^2/kN
Saturated volumetric water content	θ_w	0.35	-
Anisotropy ratio	K'_y/K'_x	1	-
Rotation angle	α	0	Degrees

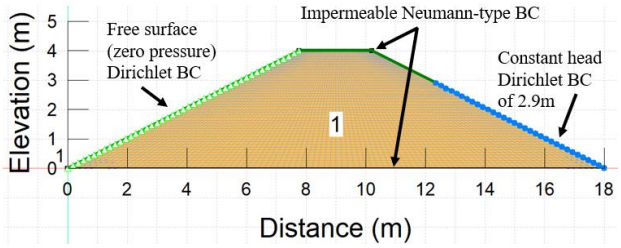

Figure 5. Geometry, mesh, and boundary conditions of SEEP/W model.

5 RESULTS AND DISCUSSION

Analysis of the results focuses on the temporal hydro-mechanical response of the levee system before and after the defect in the culvert was exposed.

5.1 Pore pressure generation prior to culvert defect exposure

The levee was saturated until the wetting front advanced past the culvert defect as measured by the pore pressure transducers. To access the saturation level of the centrifuge model, the numerical model was run until the saturated conditions reached steady state assuming no seepage at the base of the model.

After maintaining the water height for 30 minutes in Test 2, the pore pressures from PPT A and PPT B were 13.8kPa and 20.7kPa, respectively. The pore pressures were 18.9kPa and 23.5kPa at the same locations in the SEEP/W model. The centrifuge test pore pressures were 73% to 88% of the pore pressures of the numerical model. The numerically modelled and measured pore pressure and phreatic surface are shown in Figure 6 for comparison. Given time constraints, system equilibrium (i.e. the wetting front advancing to the levee toe) was not fully realized in the experimental case, contributing to the differences in the phreatic surface and pressures. However, given the similarities in shape and pressure, the wetting front was considered sufficiently advanced to justify exposing the defect.

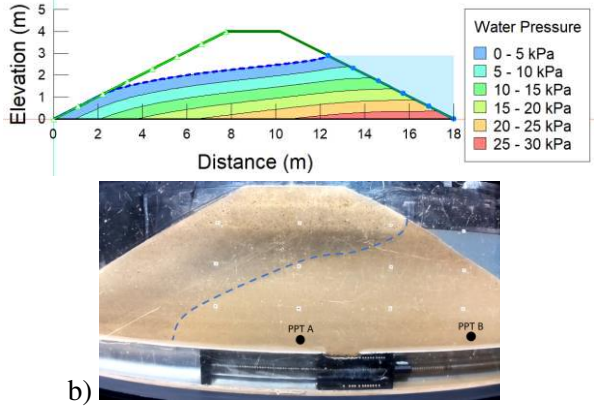

Figure 6. a) Pore pressures and phreatic surface from SEEP/W steady state analysis assuming no seepage occurs

along the culvert. b) Raspberry Pi camera imagery during saturation from Test 2 with the approximate phreatic surface indicated by a blue dashed line.

5.2 Pore pressure generation during erosion channel progression

A zone of zero pressure was created when the culvert defect was exposed. This changed the flow path and subsequently, observed pore pressures within the system; however, no abrupt changes in pore pressures were observed during plug retraction. Figure 7 presents the normalized total head at three PPT locations as a function of time until the erosion progressed to the surface for Tests 2 and 4.

To calculate the total head, a datum was set at the base of the levee. Using prototype scaling, the elevation head included the nominal g level but not the radial g effect which was considered negligible given the centrifuge size. The pressure head was calculated by dividing the pore water pressure measured by the PPTs by the unit weight of water. Note that the total head was normalized to the total head of the free water to account for variable water levels between experiments.

Time was defined relative to the exposure of the culvert defect and failure of the levee (i.e., the point when the defect was opened to manifestation of the erosion channel at the soil surface). The coloured labels for the PPTs in Figure 3 correspond to the colours used in Figure 7.

Inspection of the temporal total head in Figure 7a shows that there was not a significant change in the total head during the erosion process despite the evolution of the erosion channel. The limited total head variation in Test 2 is likely due to the placement of the instruments, which were three culvert diameters away from the defect location. The erosion channel was anticipated to progress further in the out-of-plane direction than it did, indicating that this mechanism was more localized.

Therefore, in Test 4, the PPTs were moved to only one culvert diameter away from the defect location. In Figure 7b, there is more initial variation in head at the time of the defect opening. Additionally a decrease in total head at 25% of surface manifestation can be identified, indicating head loss near the defect location despite maintained free water levels as indicated by the inset plot. This result shows that head loss within a levee section may indicate internal erosion progression. It also indicates that instrument placement needs to be sufficently close to potential seepage areas, within about one culvert diameter.

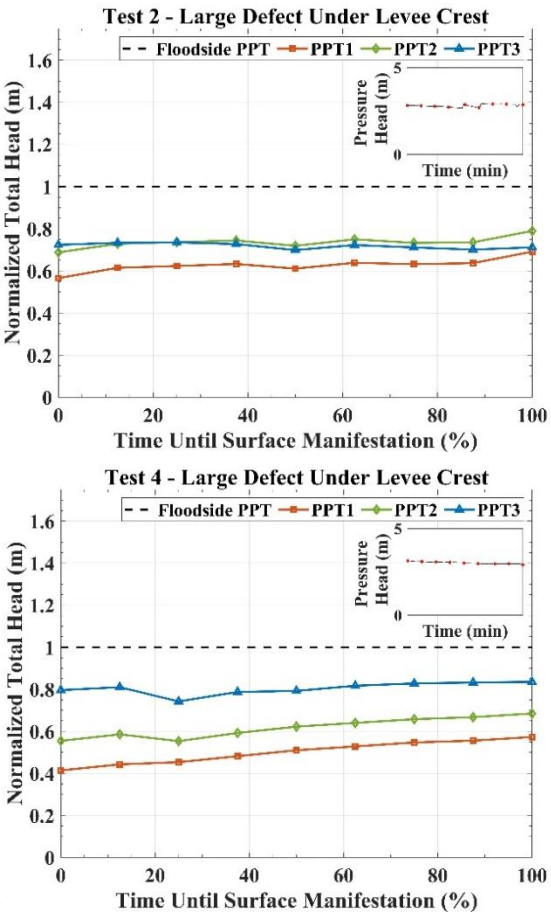

Figure 7. Normalized total head as a function of time until surface manifestation around the culvert defect for a) Test 2 where limited head loss was detected and b) Test 4. Head loss near the defect location at 25% time can be identified despite maintained free water levels.

5.3 Soil cavity propagation to the surface

Figure 8 provides an elevation view of the four tests after 60 minutes had passed (Test 1) or at the instance the erosion channel reached the surface (Test 2-4). In Test 1, a very small soil cavity formed and stabilized without propagation to the surface. This observation prompted the enlargement of the culvert defect in subsequent experiments. Upon opening the culvert defect in Test 2, an erosion channel was formed from which the soil gradually eroded. However, even with the observed surface propagation, substantial repairs would still be necessary to ensure the continued functionality of the levee for the Test 2-4 erosion scenarios.

The erosion channel in Test 2 propagated upward from the culvert defect until it reached the soil surface after 42.87min (model time). Test 3 displayed similar behaviour with surface propagation taking 25.62min. Breakthrough of the erosion channel during Test 3 took 60% of the time it took in Test 2. This can be attributed to two factors: (1) a shorter pathlength from the culvert defect to the soil surface, and (2) a

higher total head above the defect. Test 4 took 76.57min which was much longer than Test 2 despite the same defect size and position. This is due to the lack of drainage and thus transportation of fines through the culvert. The fine material was able to pile up and plug the defect, limiting flow (Fig. 8d). In test 2-4 the RealSense depth camera did not capture any surficial deformation until the erosion channel had reached the surface. However, when looking at the cross sections, it is clear the structural integrity of the levee was compromised long before any visible issues occurred at the surface. This holds particular significance for inspection results; a lack of surficial deformation prior to the erosion channel reaching the surface poses a significant challenge in proactively detecting a problem.

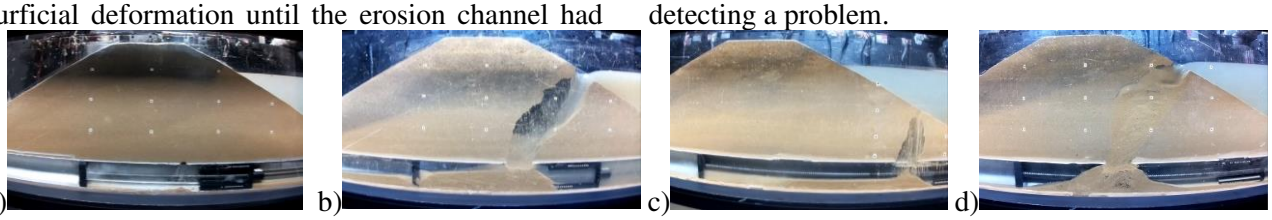

Figure 8. a) Test 1: A very small erosion channel forms and stabilizes without propagating to the surface. For figures b-d, the times between plug pull and surface propagation are reported in model time. b) Test 2: 42.87min c) Test 3: 25.62min d) Test 4: 76.57min.

6 CONCLUSIONS

This work focused on assessing the hydro-mechanical behaviour of a levee system in response to internal erosion into a buried culvert. Utilizing the ERDC Centrifuge, four 20g tests were conducted, each simulating different culvert defect scenarios. Thermal infrared sensing, a novel addition to centrifuge experiments, was demonstrated as a potential tool in future modelling efforts. Simulations performed with SEEP/W were used to approximate the levee's phreatic surface at steady state and guide when to expose the culvert defect during the physical experiments. The normalized total head during the erosion process exhibited some variations only when the sensors were within one culvert diameter away from the defect location, indicating the failure mechanism was localized. The lack of surficial deformation before surface manifestation highlights the difficulty of identifying a problem solely through surface observations. This is particularly crucial for inspectors assessing levee conditions and maintenance requirements. Additional investigation involving the systematic variation of boundary conditions and careful consideration of instrument proximity is imperative to augment the understanding of this work.

ACKNOWLEDGEMENTS

This work was supported under PE 031398, Project 511188-FY23 "Automate Inspection of Flood Control Systems (FCS)". The authors gratefully acknowledge Clint Barela and Ryan Bockman for their invaluable contributions to the fabrication of these experiments. Furthermore, the authors extend sincere appreciation to their collaborators at Virginia Tech, especially Assistant Professor Alba Yerro Colom, whose contributions played a crucial role in deciding culvert defect size for these experiments.

REFERENCES

Bowman, A., Westcott, J., & Barela, C. (2022). History, Renovation and the Future of the Centrifuge Research Complex at the US Army Corps Engineer Research and Development Center. In *ICPMG 2022 10th International Conference on Physical Modelling in Geotechnics*, 19-23 September 2022, KAIST, Daejeon, Korea.

GeoStudio. (2022). *Heat and Mass Transfer Modelling with GeoStudio* (Version 1.0). User Manual.

Horachek, P., Bransby, M. F., Hallett, P. D., & Bengough, A. G. (2009). Centrifuge modelling of climatic effects on clay embankments. *Proceedings of the Institution of Civil Engineers - Engineering Sustainability, 162*(2), 91-100. https://doi.org/10.1680/ensu.2009.162.2.91

Nakashima, K., Black, J.A., Khan, I.U., Bayton, S. (2020). Effects of Internal Erosion on Levee Instability. In: Duc Long, P., Dung, N. (eds) Geotechnics for Sustainable Infrastructure Development. Lecture Notes in Civil Engineering, vol 62. Springer, Singapore. https://doi.org/10.1007/978-981-15-2184-3_124

Ovalle-Villamil, W., & Sasanakul, I. (2021). Assessment of centrifuge modelling of internal erosion induced by upward flow conditions. *International Journal of Physical Modelling in Geotechnics, 21*(5), 251-267. https://doi.org/10.1680/jphmg.20.00004.

U.S. Army Corps of Engineers. (2018). *Levee Portfolio Report*. U.S. Army Corps of Engineers Levee Safety.

U.S. Army Corps of Engineers. (2020). *Conduits, culverts and culverts associated with dams and levee systems.* Technical report. Publication Number EM 1110-2-2902.

Vollmer, M., & Möllmann, K.-P. (2018). Infrared thermal imaging – Fundamentals, research and applications (2nd ed.). Wiley.